Journal of Power Sources 185 (2008) 159–165

Contents lists available at ScienceDirect

Journal of Power Sources

journal homepage: www.elsevier.com/locate/jpowsour

Preparation of platinum nanoparticles on carbon black with mixed binary surfactants: Characterization and evaluation as anode catalyst for low-temperature fuel cell

Dong-Ha Lim[a], Weon-Doo Lee[a], Dong-Hyeok Choi[a], Dal-Ryung Park[b], Ho-In Lee[a,*]

[a] Department of Chemical and Biological Engineering and Research Center for Energy Conversion and Storage, Seoul National University, Seoul 151-744, Republic of Korea
[b] Center for Gas Utilization Technology, KOGAS R&D Center, Ansan, Kyunggi 425-150, Republic of Korea

ARTICLE INFO

Article history:
Received 29 January 2008
Received in revised form 20 April 2008
Accepted 15 May 2008
Available online 4 July 2008

Keywords:
Low-temperature fuel cell
Colloidal method
Surfactant
Electrocatalysts
Platinum nanoparticles

ABSTRACT

Platinum nanoparticles supported on Vulcan XC-72R prepared by a surfactant-stabilized colloidal method exhibit excellent properties as an anode catalyst for a low-temperature fuel cell. A Pt/C catalyst prepared with a 10-fold critical micelle concentration of mixed non-ionic surfactants [polyoxyethylene (23) lauryl ether + polyoxyethylene (20) sorbitan monolaurate (Brij 35 + Tween 20)] shows the highest catalytic activity and the greatest electrochemical surface-active area among those prepared. The maximum current density of this catalyst is much higher than that of a commercial Pt/C catalyst (E-TEK). Moreover, X-ray diffraction and transmission electron microscopy analyses reveal that Pt/C prepared with Brij 35 + Tween 20 has an average particle size of 2.4 nm with quite a narrow distribution between 2 and 3 nm, which is the smallest among all the catalysts prepared. This is attributed to the formation of more compact micelles. Mixtures of non-ionic and anionic surfactants result in less compact micelles.

1. Introduction

Fuel cells are attractive for electric power generation, portable power and electric vehicle applications owing to their high efficiency and low pollutant emissions [1]. These systems are usually classified as low- or high-temperature fuel cells according to their operating temperature. Low-temperature fuel cells operating at 60–100 °C include proton-exchange membrane fuel cells (PEMFCs) and direct methanol fuel cells (DMFCs). Despite advantages such as low operating temperature and high specific energy, many obstacles have to be overcome to realize commercial applications [2–5].

The best electrocatalyst identified so far for low-temperature fuel cell is Pt metal on carbon. Platinum is expensive, however, so its loading must be minimized without weakening the catalytic activity. Thus, there has been great focus on synthesizing Pt nanoparticles on carbon to maximize surface availability and improve catalytic activity [6–20]. Synthesis methods include colloidal [9–11] and electrochemical methods [12], alcohol reduction [13,14], reverse micellization [15–17], photoreduction [18], and metal-organic chemical vapour deposition [19]. It is difficult to control the particle size in most of these methods, whereas the surfactant-stabilized colloidal method is suggested to show better control [21,22]. Platinum colloid systems comprised of a metallic core and a surfactant shell have been investigated [22]. This method [9–11] has been widely used in the preparation of metal colloids for homogeneous catalysis, whereby well-dispersed nanometal colloids can be formed and stabilized in aqueous solution in the presence of a surfactant via a steric mechanism [23,24]. Fig. 1 illustrates the general scheme for surfactant stabilization in the preparation of metal nanoparticles deposited on carbon. The process involves: (i) synthesizing surfactant-stabilized Pt colloids as a core-shell structure; (ii) depositing surfactant-stabilized Pt colloids on a carbon support; and (iii) removing the surfactant by washing to yield well-dispersed Pt particles on the carbon support. Using a single surfactant typically results in Pt nanoparticles of 3–5 nm size with moderate dispersion of Pt on carbon [22]. Therefore, it is necessary to explore more effective methods for preparing smaller Pt nanoparticles on carbon with better dispersion. One promising alternative is mixed binary surfactants, which show unique interfacial and micellization behaviour [25]. While single surfactants have been extensively investigated, few studies have considered mixed surfactant systems for the preparation of Pt metal colloids, to the best of our knowledge.

Platinum metal colloids obtained by chemical reduction of their salts in solution can be stabilized by suitable surfactants as a core-shell structure to prevent aggregation of the metal nanoparticles [21,22]. Catalysts of metal nanoparticles with a narrow size-distribution have also been obtained by the colloidal method

* Corresponding author. Tel.: +82 2 880 7072; fax: +82 2 888 1604.
E-mail address: hilee@snu.ac.kr (H.-I. Lee).

0378-7753/$ – see front matter © 2008 Elsevier B.V. All rights reserved.
doi:10.1016/j.jpowsour.2008.05.092

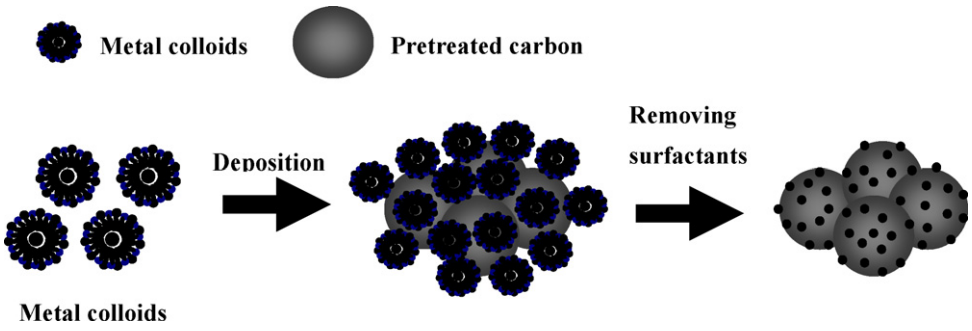

Fig. 1. Schematic illustration of colloidal method to prepare Pt/C catalysts.

[21,22]. Micelles usually form above a certain surfactant concentration – the critical micelle concentration (CMC) [26] – which determines the concentration of micelles available for metallic particle nucleation. In addition, micelle shape is influenced by various factors, including the surfactant concentration and type, the choice of solution, and environmental conditions such as the hydrophobic volume, chain length, head group area, etc. [26]. The mechanisms responsible for micelle dispersion in solution are divided into three classes, namely: electrostatic stabilization, steric stabilization, and electrostatic-steric stabilization. For colloids of metal particles, stabilization has been attributed to the interaction of repulsion and attraction forces among the particles [23,24].

The objective of this study is to prepare well-dispersed Pt nanoparticles to enhance the performance of low-temperature fuel cell. Platinum nanoparticles are prepared on carbon by a colloidal method using mixed binary surfactants and are then evaluated for methanol oxidation. The Pt precursor exhibits almost complete loading on the carbon with excellent dispersion when mixed binary surfactants at a concentration of ten times the CMC (or 10× CMC) are employed. Samples are characterized using high-resolution transmission electron microscopy (HR-TEM), X-ray diffraction (XRD), H_2 adsorption/desorption measurements, and chronoamperograms.

2. Experimental

2.1. Pt/C electrocatalysts

The Pt/C catalysts were synthesized by a colloidal method using mixed binary surfactants. The loading amount of Pt metal in the experimental and commercial (E-TEK) catalysts was fixed at 20 wt.%. Polyoxyethylene (23) lauryl ether (Brij 35, Sigma–Aldrich) and polyoxyethylene (20) sorbitan monolaurate (Tween 20, Samchun Chemicals) were used as non-ionic surfactants, and sodium dodecyl sulfate (SDS, Acors Organics) as an anionic surfactant, to stabilize the preparation of Pt metal colloids. Chloroplatinic acid ($H_2PtCl_6{\bullet}6H_2O$, Acros Organics) was used as the Pt precursor.

To prepare the catalysts, 0.066 g (1.60×10^{-4} mol) $H_2PtCl_6{\cdot}6H_2O$ was added to 100 ml deionized water containing 9.20×10^{-5} mol Brij 35 and 8.04×10^{-5} mol Tween 20. Under vigorous stirring, 0.01 g (2.64×10^{-4} mol) sodium borohydride ($NaBH_4$, Junsei), a strong liquid-phase reducing agent, in 50 ml of deionized water was injected into the metal salt solution in a drop-wise manner at 1 ml min^{-1} using a 50 ml syringe. The colour of the solution changed immediately to black after the addition of the reducing agent [27,28] and resulted in the formation of nano-sized and well-dispersed, surfactant-stabilized, Pt colloids. Then 0.1 g of carbon black powder (Vulcan XC-72R, Cabot Co.), which was pretreated with 60% nitric acid at its boiling point (140 °C) [29,30], was dispersed in methanol and then added to the surfactant-stabilized colloidal metal solution. After stirring for 6 h, the resultant suspension was filtered and washed with ethanol and hot distilled water (about 80 °C) to remove completely residual chloride and surfactant, which negatively affect the catalytic activity. The remaining powder was dried overnight in a vacuum oven at room temperature.

2.2. Physical characterization

The surface morphology of Pt nanoparticles on the surface of carbon black was studied by HR-TEM (JEM-3010, JEOL) at 300 kV. The catalyst was dispersed in ethanol by ultrasonication, and TEM samples were prepared by placing a drop of the suspension on a copper grid covered with a carbon film followed by evaporation of the ethanol. Particle-size distribution of the Pt nanoparticles on carbon was obtained by measuring the sizes of 150 Pt particles inside a TEM image. Structural characteristics of the powders were investigated by XRD (D8 ADVANCE, Bruker) using Cu Kα radiation. The working voltage and current were maintained at 40 kV and 30 mA, respectively. The range $2\theta = 20–80^\circ$ was scanned at a rate of 2° min^{-1}. TG-DSC measurements were conducted on a thermal analyzer (SDT Q-600, TA Instruments) at 30–800 °C with an air flow of 100 ml min^{-1} and using an alumina sample pan.

2.3. Electrochemical activity

Electrochemical measurements were carried out in a half-cell test using a potentiostat (PC4/750, Gamry Instruments). The catalyst ink was prepared by mixing catalyst particles with 5% Nafion® solution (ratio of 3:1; 1100 EW, Du Pont) and isopropyl alcohol by ultrasonication for 30 min. A glassy carbon (GC) disc electrode (MF-2012, BAS; Ø 6 mm) was polished to a mirror finish with a 0.05 μm-sized γ-alumina suspension (40-6301-016, Buehler) before each experiment and was used as the substrate. A drop of catalyst ink was pipetted on to the surface of the GC disk electrode and dried at room temperature. Each electrode was installed in a three-electrode cell with a platinum mesh electrode (219810, Princeton Applied Research) as the counter-electrode and a KCl saturated Ag|AgCl electrode (MF-2052, Bioanalytical Systems) as the reference electrode, which was located as close as possible to the working electrode. The cell was filled with electrolyte and purged with N_2 to remove dissolved oxygen. All potentials were recorded with respect to the standard hydrogen electrode (SHE). Before electrochemical measurements, a set of potential cycles [(between +0 and 1.2 V (vs. SHE) at 100 mV s^{-1})] were applied to the electrode for surface cleaning and to obtain an active electrochemical surface.

3. Results and discussion

3.1. Preparation and physical characterization

The Pt/C catalysts are synthesized by a colloidal method with borohydride reduction in aqueous solution containing mixed binary surfactants as, shown in Fig. 1. In this colloidal method, chemical reduction of the Pt precursor to a metallic Pt colloid proceeds rapidly on the addition of $NaBH_4$ solution, and is clearly observed by the colour change of the precursor solution. Surfactant-stabilized Pt colloids can be formed and stabilized in aqueous solution containing the mixed binary surfactants [31]. The stabilization mechanism of mixed binary surfactants in aqueous solution is related to a steric effect with the hydrophobic tail of the surfactant orienting towards the Pt particles and the hydrophilic head pointing towards the aqueous solution. The Pt colloids can be immobilized on to the hydrophilic carbon surface since the hydrophilic parts of the Pt colloids are strongly attached to the hydrophilic surface of the pretreated carbon. Treatment of carbon black with boiling nitric acid is known to increase the hydrophilicity [29,30]. Finally, an outstanding dispersion of the Pt particles is obtained on the carbon support through the washing procedures described in Section 2.

Three combinations of surfactants are employed in this study: Brij 35 + Tween 20, Brij 35 + SDS, and Tween 20 + SDS (named as B + T, B + S, and T + S, respectively). These surfactants have identical hydrophobic tails of 12 methylene groups, but different types and sizes of hydrophilic head groups. The chemical formulae of the surfactants are listed in Table 1. The CMC values of Brij 35, Tween 20 and SDS are 9.20×10^{-5}, 8.04×10^{-5} and 8.40×10^{-3} mol L^{-1}, respectively [32]. According to Tamizhmani et al. [32], the CMC of a mixed binary surfactant, CMC_M, can be calculated as:

$$\frac{1}{CMC_M} = \frac{\alpha}{CMC_x} + \frac{1-\alpha}{CMC_y} \quad (1)$$

where α and $1-\alpha$ are the mole fractions of surfactants x and y in the mixture, respectively. CMC_x and CMC_y are the CMC values for pure surfactants x and y. CMC_M values calculated from Eq. (1) for B + T, B + S and T + S are 8.58×10^{-5}, 1.59×10^{-4} and 1.82×10^{-4} mol L^{-1}, respectively.

The Pt/C samples prepared with mixed binary surfactants at 10 × CMC were characterized by means of XRD (Fig. 2). The diffraction peaks at 39, 46, 68 and 81° are attributed to the Pt(1 1 1), (2 0 0), (2 2 0) and (3 1 1) crystalline planes, respectively, which correspond to typical Pt crystals with a face-centered cubic structure. This demonstrates that the platinum precursor is successfully reduced. The broad peak near $2\theta = 25°$ is attributed to carbon black. Average crystallite sizes for the Pt/C catalysts are obtained from the full width at half-maximum (FWHM) and the angular position of the Lorentzian-fitted (1 1 1) peak using Scherrer's equation [33], as summarized in Table 2. The Pt/C samples prepared with B + T, B + S, and T + S have crystallite sizes of approximately 2.5, 4.7, and 7.2 nm, respectively. The B + T mixture at 10× CMC yields the smallest Pt particles. Surfactant concentration strongly influences the Pt particle size [34]. At a concentration of 50× CMC, mixed binary surfactants cause serious aggregation of Pt particles, which results in much larger metal particles. It is considered that this is due to the formation of cylindrical micelles caused by excess surfactant, as discussed below.

Table 1
Chemical formule of surfacatants

Sample	Formula
Polyoxyethylene (23) lauryl ether (Brij 35)	$C_{12}H_{25}(CH_2CH_2O)_{23}OH$
Polyoxyethylene (20) sorbitan monolaurate (Tween 20)	$C_{58}H_{14}O_{26}$
Sodium dodecyl sulfate (SDS)	$C_{12}H_{25}NaO_4S$

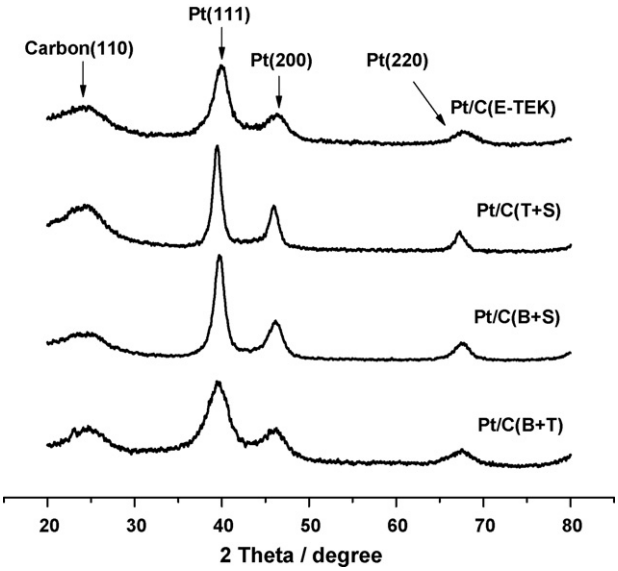

Fig. 2. X-ray diffraction patterns of Pt/C catalysts prepared with mixed binary surfactants (10× CMC) and of a commercial Pt/C (E-TEK).

Table 2
Comparison of particle sizes of Pt/C catalysts prepared with 10× CMC of mixed binary surfactants and a commercial Pt/C catalyst (E-TEK)

Sample	Particle size from TEM (nm)	Particle size from XRD (nm)
Pt/C(B + T)	2.4	2.5
Pt/C(B + S)	5.2	4.7
Pt/C(T + S)	7.0	7.2
Pt/C(E-TEK)	3.5	3.3

Different CMC values of surfactants can be explained by the role of the surfactant during Pt reduction. As the surfactant concentration increases, spherical micelles are converted to cylindrical micelles (Fig. 3). Fig. 4a shows the particle size and dispersion for the Pt/C sample prepared with B + T at 10× CMC. The majority of the Pt particles are in the range 2–3 nm, with a narrow particle-size distribution. As shown in a HR-TEM image (Fig. 4b), Pt nanoparticles are dispersed mainly on the surface of each grain of the carbon support. The particle-size distribution of the Pt nanoparticles on carbon is obtained by directly measuring the sizes of 150 randomly chosen particles in Fig. 4a. The result is illustrated in Fig. 4c. The Pt nanoparticles are in the range of 1–4 nm with a relatively narrow particle size-distribution between 2 and 3 nm and an average size of 2.4 nm. When mixed binary surfactants at 5× CMC are applied, high dispersion is obtained (data not shown), but not at 10× CMC.

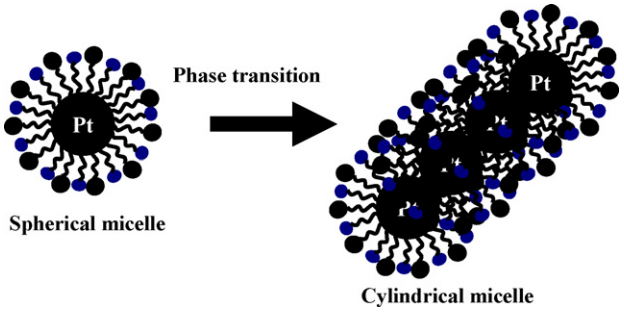

Fig. 3. Phase transition of micelle structures with different CMC.

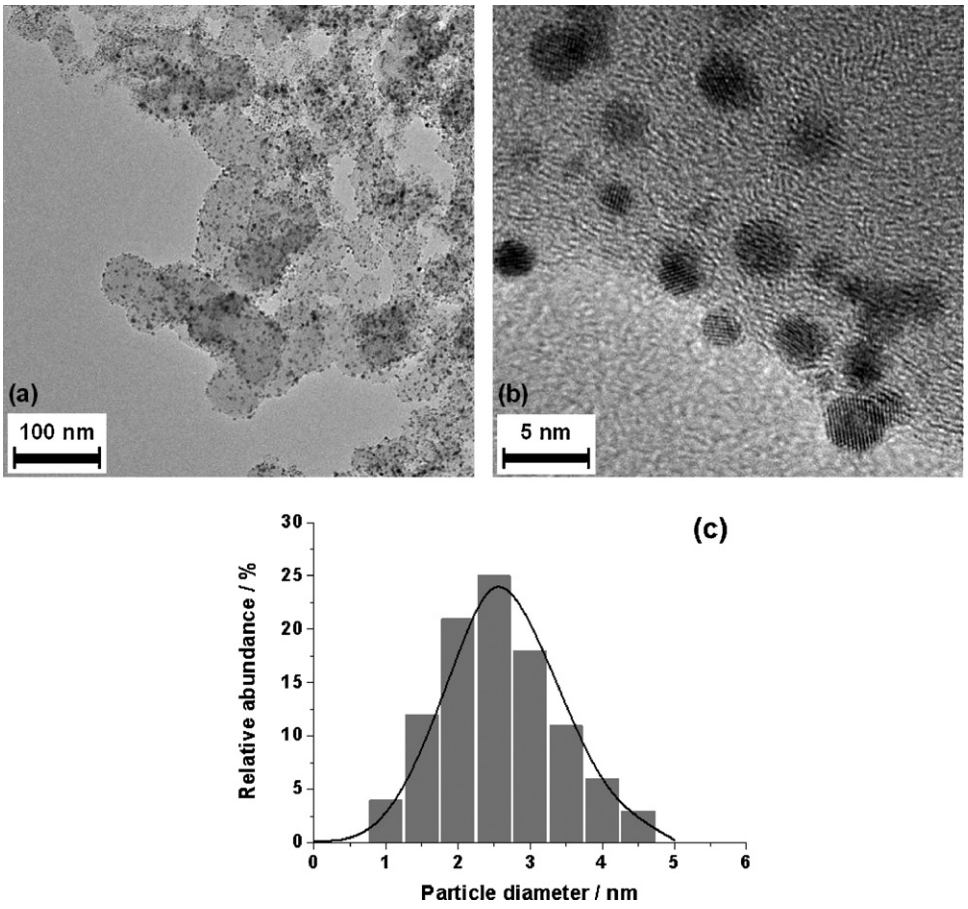

Fig. 4. (a) TEM image, (b) enlarged HR-TEM image and (c) particle-size distribution of Pt/C catalyst prepared with 10× CMC of B + T.

When the concentration is increased to 50× CMC, severe aggregation of Pt nanoparticles occurs, as witnessed in Fig. 5a. At 10× CMC, Pt nanoparticles are surrounded by surfactants to form spherical micelles, which inhibit aggregation (Fig. 4b). When the surfactant concentration becomes too high, spherical micelles are converted to cylindrical micelles and form tubular-shaped Pt nanoparticles (Fig. 5b). The average size of the Pt nanoparticles is estimated from TEM images and compared with the average XRD crystallite size of Pt, as shown in Table 2. The average TEM particle size agrees well with the average crystallite size determined from broadening of the (111) diffraction peak, which implies that the Pt particles are mostly single-crystalline. The particle size of the Pt/C catalyst prepared with the mixed non-ionic surfactants (B + T) is smaller than those of the catalysts prepared with mixed non-ionic and anionic surfactants (B + S, T + S). It is considered that this is due to the formation of more compact spherical micelles in the presence of B + T instead of

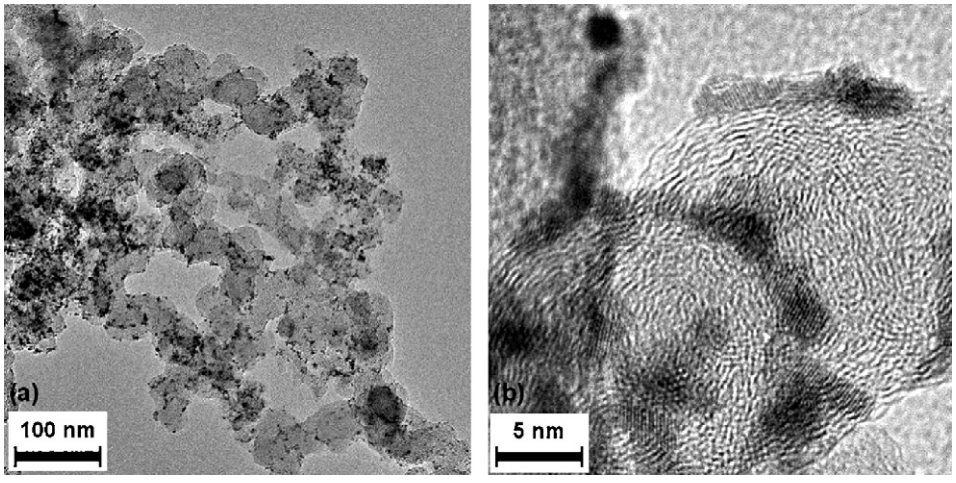

Fig. 5. (a) TEM image and (b) enlarged HR-TEM image of Pt/C catalyst prepared with 50× CMC of B + T.

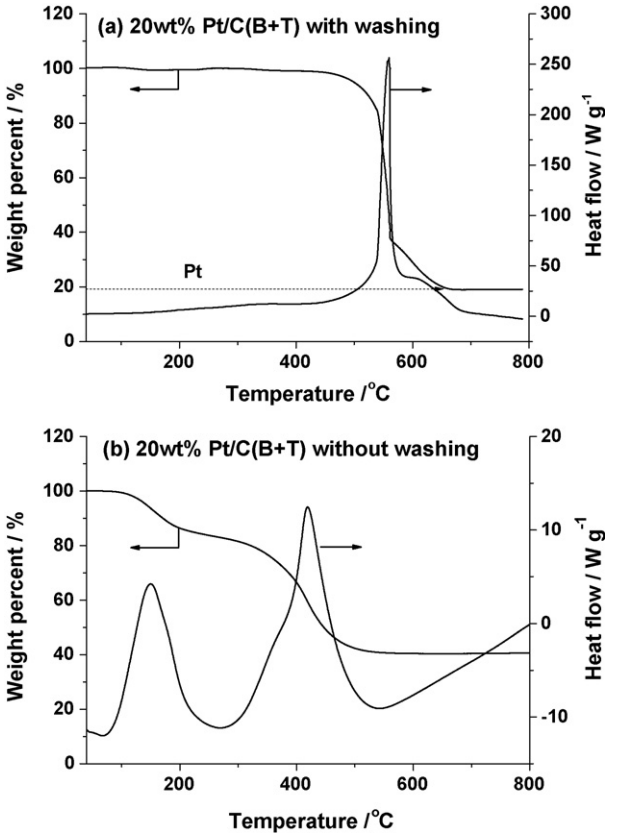

Fig. 6. TG-DSC curves of Pt/C catalyst prepared with 10× CMC of B+T: (a) with washing; (b) without washing.

B + S and T + S. Since repulsive interaction among DS^- anions would make spherical micelles of the latter two less compact, as discussed by Ghosh and Moulik [23], catalyst particles prepared with the B + S and T + S surfactant mixtures are expected to be larger than those prepared with the B + T surfactant.

In the above colloidal method, chemical reduction of Pt ions to a metallic Pt colloid proceeds rapidly on $NaBH_4$ addition, as clearly observed by the colour change of the precursor solution [27,28]. TG-DSC analysis is used to check for complete reduction of the Pt precursor and the complete removal of surfactants. Fig. 6a shows the TG-DSC curve of the 20 wt.% Pt/C catalyst after washing and drying. The strong endothermic reaction with significant weight loss starting at ~400 °C is due to the combustion of carbon. The combustion is complete at ~650 °C leaving 19.1 wt.% components as a residue, which is the loading of Pt metal. It is clear that the preparation method results in complete reduction of Pt and full loading of Pt nanoparticles on the carbon. The shoulder of the weight loss peak at 600 °C is thought to correspond to different states of carbon. No other weight loss peak is observed and therefore suggests that the washing and drying process is sufficient to remove surfactants and inorganic salts. To confirm this conclusion, comparative TG-DSC studies were carried out on a 20 wt.% Pt/C sample without washing (Fig. 6b), and that was filtered and dried in a vacuum oven. Three weight loss peaks are observed. The first strong endothermic peak at ~150 °C appears to correspond to the Pt-catalyzed oxidation of alcohols formed from Pt-catalyzed decomposition of the surfactant. The second should arise from oxidation of carbon. The temperature is, however, drastically shifted to lower values compared with washed Pt/C. Consequently, inorganic salts are believed to play a role in the oxidation reaction. After complete oxidation, there is a 40 wt.% residue of Pt and inorganic salts.

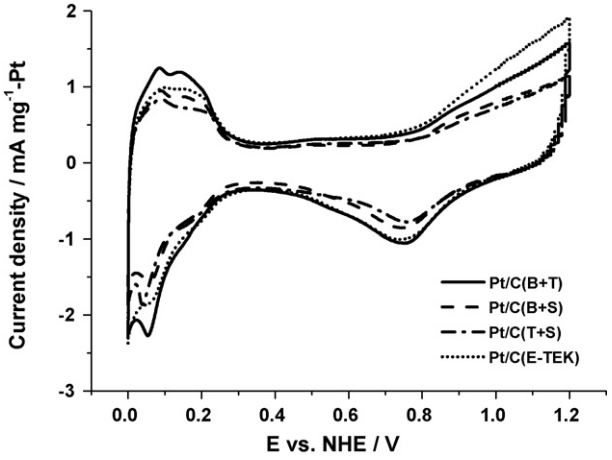

Fig. 7. Cyclic voltammograms of H_2 adsorption/desorption on Pt/C prepared with 10× CMC of mixed binary surfactants and a commercial catalyst (E-TEK) in 0.5 mol L^{-1} H_2SO_4 at 25 °C (scan rate = 20 mV s^{-1}).

3.2. Electrochemical measurements

To measure H_2 adsorption/desorption curves, the potential was cycled between 0 and 1.2 V (vs. SHE) at 20 mV s^{-1} in 0.5 mol L^{-1} H_2SO_4 purged with nitrogen at 25 °C. Adsorption and desorption curves for Pt/C catalysts prepared with mixed binary surfactants (10× CMC) are shown in Fig. 7. The curves are stabilized after 10 cycles in the potential range. The catalysts exhibit well-defined H_2 adsorption/desorption peaks in the potential region 0–0.25 V (vs. SHE) and adsorption/desorption peaks for O_2 species at ~0.7 and 1.0 V (vs. SHE), these are in good agreement with literature values [35,36]. The electrochemically active surface area (EAS) of Pt/C catalysts is estimated using the integrated charge in the H_2 desorption region according to Gasteiger et al. [37]:

$$\text{EAS}\,(\text{m}^2\,\text{g}^{-1}) = \frac{Q_H}{0.21} \times [\text{Pt}] \quad (2)$$

where Q_H (mC cm^{-2}) is the charge exchanged during hydrogen desorption on the Pt surface, [Pt] (mg cm^{-2}) is the Pt loading on the electrode, and 0.21 is the charge required to oxidize a monolayer of hydrogen on the Pt surface.

The EAS calculated for the Pt/C catalyst prepared with 10× CMC of B + T is higher than those for the catalysts prepared with 10× CMC of B + S, T + S and also for the commercial catalyst (E-TEK) (Table 3). This indicates that the high EAS value is due to the presence of well-dispersed Pt nanoparticles on the carbon support, as witnessed in TEM images (Fig. 4).

Evaluation of the catalysts for methanol oxidation is carried out by using an electrolyte comprised of a mixed solution of 2 mol L^{-1} CH_3OH and 0.5 mol L^{-1} H_2SO_4 purged with nitrogen at 40 °C. The current values are normalized with respect to both the Pt loading and the surface area since methanol adsorption and dehydrogenation occur only at Pt sites at room temperature [38–40]. The EAS of

Table 3
Electrocatalytic characteristics of Pt/C catalysts prepared with 10× CMC of mixed binary surfactants and of a commercial catalyst (E-TEK)

Sample	Mass activity[a] (mA mg_{Pt}^{-1})	Area activity[a] (mA cm_{Pt}^{-2})	EAS[b] ($m^2\,g^{-1}$)
Pt/C(B+T)	313.3	0.732	42.8
Pt/C(B+S)	219.0	0.615	35.6
Pt/C(T+S)	171.4	0.579	29.6
Pt/C(E-TEK)	264.6	0.711	37.2

[a] The activity data were taken from the CVs shown in Fig. 8.
[b] The EAS data were taken from the CVs shown in Fig. 7.

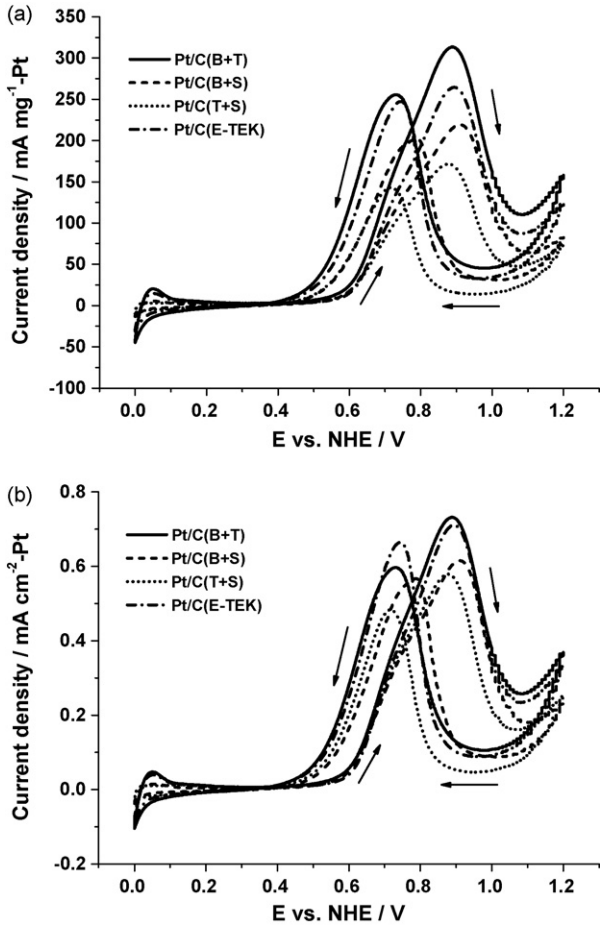

Fig. 8. (a) Mass and (b) area normalized cyclic voltammograms for methanol oxidation by Pt/C catalysts prepared with 10× CMC of mixed binary surfactants and by a commercial catalyst (E-TEK) in 2 mol L^{-1} CH_3OH + 0.5 mol L^{-1} H_2SO_4 at 40 °C (scan rate = 20 mV s^{-1}).

Pt metal is calculated from the desorption of hydrogen using Eq. (2). The mass- and area-normalized current densities are given in Fig. 8. The current density is generally normalized by the metal loading ($mA\,mg_{Pt}^{-1}$) to compare the activity of different catalysts in terms of economic efficiency. The Pt/C catalyst prepared with 10 × CMC of B + T gives the highest activity in terms of mass–current density for methanol oxidation. Even though the mass–current density represents the economic efficiency of a catalyst, it does not take into account the surface area of active metal sites. Consequently, the area-normalized current density is required to represent the intrinsic activity of active sites on an electrocatalyst. Area-normalized current densities for methanol oxidation on Pt/C catalysts are presented in Fig. 8b. Catalyst performance is ranked in the same order for mass- and area-normalized current densities. The onset potential for methanol oxidation is ~0.55 V (vs. RHE) on all the Pt/C catalysts. Although the catalyst prepared with B + T exhibits the highest activity than there is difference in the mass-normalized and the area-normalized current densities that is actually due to a difference in metal dispersion. The electrocatalytic activities for methanol oxidation are summarized in Table 3.

Chronoamperograms of Pt/C catalysts prepared with mixed binary surfactants in 2 mol L^{-1} CH_3OH and 0.5 mol L^{-1} H_2SO_4 purged with nitrogen at 40 °C at 0.55 V (vs. NHE) are presented in Fig. 9. The results reveal higher performance for the Pt/C catalyst prepared with B + T than for the other catalysts. The oxidation current density of a commercial catalyst (E-TEK) experiences a rapid

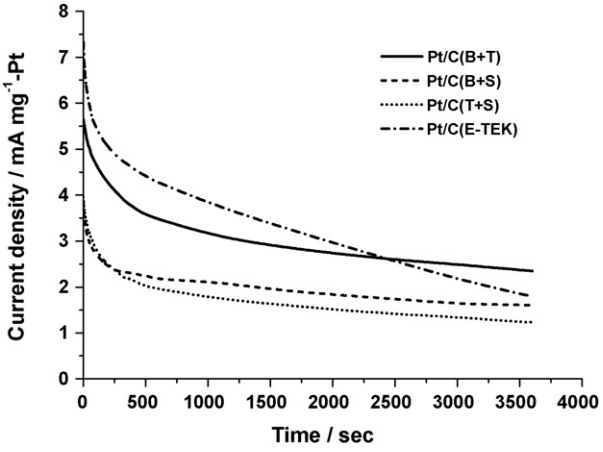

Fig. 9. Chronoamperograms of Pt/C catalysts prepared with 10× CMC of mixed binary surfactants and a commercial Pt/C (E-TEK) at 0.55 V (vs. SHE) in 2 mol L^{-1} CH_3OH + 0.5 mol L^{-1} H_2SO_4 at 40 °C (scan rate = 20 mV s^{-1}).

decrease with time even though the initial current density is better. On the other hand, the Pt/C catalyst prepared with B + T shows an initial current drop in the first 500 s, followed by a slower decay. This significant improvement in catalyst performance is attributed to better Pt utilization by the well-dispersed catalyst nanoparticles on the carbon support. The chronoamperometric results agree well with the trends for methanol oxidation.

4. Conclusions

Highly dispersed Pt nanoparticles have been successfully prepared via a colloidal method using Vulcan XC-72R as a support. Studies with TEM and XRD reveal that well-dispersed Pt nanoparticles on carbon prepared with mixed binary surfactants at 10 × CMC are approximately 2–3 nm in diameter and are almost single crystalline. This catalyst also gives the best catalytic activity and highest EAS compared with other catalysts, which include a commercial catalyst (E-TEK). The improvement in catalytic activity is attributed to the narrow size-distribution of Pt nanoparticles and their good dispersion on the carbon support. This study demonstrates that colloidal methods using surfactants represent a promising route to the realization of highly active electrocatalysts for low-temperature fuel cells.

Acknowledgements

This work was financially supported by the Korea Gas Corporation, the Brain Korea 21 Project in 2006, and the ERC Program of MOST/KOSEF (Grant No. R11-2002-102-00000-0).

References

[1] J. Larminie, A. Dicks, Fuel Cell Systems, Wiley, New York, 2000.
[2] S. Ge, X. Li, B. Yi, I.M. Hsing, J. Electrochem. Soc. 152 (2005) A1149.
[3] G. Lin, T.V. Nguyen, J. Electrochem. Soc. 152 (2005) A1942.
[4] R.F. Silva, S. Passerini, A. Pozio, Electrochim. Acta 50 (2005) 2639.
[5] T.C. Deivaraj, J.Y. Lee, J. Power Sources 142 (2005) 43.
[6] D.-H. Lim, D.-H. Choi, W.-D. Lee, D.-R. Park, H.-I. Lee, Electrochem. Solid-State Lett. 10 (2007) B87.
[7] J.-S. Choi, W.-S. Chung, H.-Y. Ha, T.-H. Lim, I.-H. Oh, S.-A. Hong, H.-I. Lee, J. Power Sources 156 (2006) 466.
[8] S.-A. Lee, K.-W. Park, B.-K. Kwon, Y.-E. Sung, J. Ind. Eng. Chem. 9 (2003) 63.
[9] M. Pan, H. Tang, S.P. Jiang, Z. Liu, J. Electrochem. Soc. 152 (2005) A1081.
[10] Z. Liu, X.Y. Ling, X. Su, J.Y. Lee, L.M. Gan, J. Power Sources 149 (2005) 1.
[11] C. Kim, H.-H. Kown, I.-K. Song, Y.-E. Sung, W.-S. Chung, H.-I. Lee, J. Power Sources 171 (2007) 404.
[12] J.C. Zoval, J. Lee, S. Gorer, R.M. Penner, J. Phys. Chem. B 102 (1998) 1166.
[13] T. Kim, M. Takahashi, M. Nagai, K. Kobayashi, Electrochim. Acta 50 (2004) 817.

[14] T. Frelink, W. Visscher, J.A.R. Van Veen, Electrochim. Acta 39 (1994) 1871.
[15] L. Xiong, A. Manthiram, Electrochim. Acta 50 (2005) 2323.
[16] M.P. Pileni, Langmuir 13 (1997) 3266.
[17] H. Sato, T. Hirai, I. Komasawa, Ind. Eng. Chem. Res. 34 (1995) 2493.
[18] J.C. Kennedy, A.K. Datye, J. Catal. 179 (1998) 375.
[19] S. Daniele, C. Bragato, G.A. Battiston, R. Gerbasi, Electrochim. Acta 46 (2001) 2961.
[20] D.-H. Lim, W.-D. Lee, D.-H. Choi, H.-H. Kwon, H.-I. Lee, Electrochem. Commun. 10 (2008) 592.
[21] J. Tanori, N. Duxin, C. Petit, P. Veillet, M.P. Pileni, Colloid Polym. Sci. 273 (1995) 886.
[22] X. Wang, I.M. Hsing, Electrochim. Acta 47 (2002) 2981.
[23] S. Ghosh, S.P. Moulik, J. Colloid Interf. Sci. 208 (1998) 357.
[24] T.J. Schmidt, M. Noeske, H.A. Gasteiger, R.J. Behm, P. Britz, W. Brijoux, H. Bönnemann, J. Electrochem. Soc. 145 (1988) 925.
[25] M. Gotz, H. Wendt, Electrochim. Acta 43 (1998) 3637.
[26] H. Bönnemann, R. Brinkmann, P. Neiteler, Appl. Organomet. Chem. 8 (1994) 129.
[27] S. Hachisu, Surfactant Science Series, vol. 15, Marcel Dekker Inc., New York, 1984, p. 147.
[28] J.R.C. Salgado, E. Antolini, E.R. Gonzalez, J. Electrochem. Soc. 151 (2004) A2143.
[29] D.-H. Lim, L. Lu, D.B. Kim, D.-H. Choi, D.-R. Park, H.-I. Lee, J. Nanopart. Res. 10 (2008) 1215.
[30] Y.H. Li, C. Xu, B. Wei, X. Zhang, M. Zheng, D. Wu, P.M. Ajayan, Chem. Mater. 14 (2002) 483.
[31] M. Kerker, J. Colloid Interf. Sci. 112 (1986) 302.
[32] G. Tamizhmani, J.P. Dodelet, D. Guay, J. Electrochem. Soc. 143 (1996) 18.
[33] V. Radmiloviae, H.A. Gasteiger, P.N. Ross Jr., J. Catal. 154 (1995) 98.
[34] T. He, E. Kreidler, L. Xiong, J. Luo, C.J. Zhong, J. Electrochem. Soc. 153 (2006) A1637.
[35] J.R.C. Salgado, E. Antolini, E.R. Gonzalez, J. Power Sources 138 (2004) 56.
[36] N.M. Markovic, H.A. Gasteiger, P.N. Ross Jr., X. Jiang, I. Villegas, M.J. Weaver, Electrochim. Acta 40 (1995) 91.
[37] H.A. Gasteiger, N. Markovi, P.N. Ross, E.J. Cairns, J. Electrochem. Soc. 141 (1994) 1795.
[38] M. Ciureanu, H. Wang, J. Electrochem. Soc. 146 (1999) 4031.
[39] L. Dubau, F. Hahn, C. Countaceau, J.-M. Leger, C. Lamy, J. Electroanal. Chem. 407 (2003) 554.
[40] Y. Takasu, T. Fujiwara, Y. Murakami, K. Sasaki, M. Oguri, T. Asaki, W. Sugimoto, J. Electrochem. Soc. 147 (2000) 4421.